

<https://helda.helsinki.fi>

---

## Hydrostannylation of Olefins by a Hydridostannylene Tungsten Complex

Zhu, Qihao

2022-11-17

---

Zhu , Q , Fettinger , J C , Vasko , P & Power , P P 2022 , ' Hydrostannylation of Olefins by a  
pÿ Hydridostannylene Tungsten Complex ' , Organometallics , vol. 41 , no

---

<http://hdl.handle.net/10138/355876>

<https://doi.org/10.1021/acs.organomet.2c00494>

---

cc\_by

publishedVersion

---

*Downloaded from Helda, University of Helsinki institutional repository.*

*This is an electronic reprint of the original article.*

*This reprint may differ from the original in pagination and typographic detail.*

*Please cite the original version.*

# Hydrostannylation of Olefins by a Hydridostannylenene Tungsten Complex

Qihao Zhu, James C. Fettinger, Petra Vasko,\* and Philip P. Power\*



Cite This: <https://doi.org/10.1021/acs.organomet.2c00494>



Read Online

ACCESS |



Metrics & More

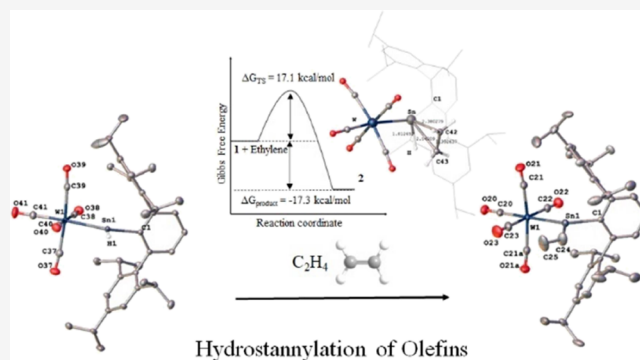


Article Recommendations



Supporting Information

**ABSTRACT:** Reaction of the aryltin(II) hydride  $\{\text{Ar}^{i\text{Pr}6}\text{Sn}(\mu\text{-H})\}_2$  ( $\text{Ar}^{i\text{Pr}6} = -\text{C}_6\text{H}_3-2,6-(\text{C}_6\text{H}_2-2,4,6\text{-}i\text{Pr}_3)_2$ ) with two equivalents of the tungsten carbonyl THF complex,  $[\text{W}(\text{CO})_5(\text{THF})]$ , afforded the divalent tin hydride transition metal complex,  $\text{W}(\text{CO})_5\{\text{Sn}(\text{Ar}^{i\text{Pr}6})\text{H}\}$ , (**1**). Complex **1** reacted rapidly with ethylene, or propylene under ambient conditions to yield the corresponding hydrostannylated organometallic species,  $\text{W}(\text{CO})_5\{\text{Sn}(\text{Ar}^{i\text{Pr}6})(\text{Et})\}$  (**2**), or  $\text{W}(\text{CO})_5\{\text{Sn}(\text{Ar}^{i\text{Pr}6})(\text{Pr})\}$  (**3**), via olefin insertion into the Sn–H bond. Treatment of **1** with the Lewis base dbu (dbu = 1,8-diazabicycloundec-7-ene) afforded the Lewis acid–base complex,  $\text{W}(\text{CO})_5\{\text{Sn}(\text{Ar}^{i\text{Pr}6})(\text{dbu})\text{H}\}$  (**4**), indicating that the Lewis acidity of the tin atom is preserved in **4**. The complexes were characterized by X-ray crystallography, and by UV–visible, FT-IR, and multinuclear NMR spectroscopies. DFT calculations suggest hydrostannylation of ethylene with **1** proceeds via coordination of ethylene to the tin atom, then insertion into the Sn–H bond. Further computational study on the reactivity of **1** toward  $\text{Ph}_3\text{SiH}$  indicated that the rate-determining step involves the metathesis reaction of a Sn–C/Si–H bond with a very high energy barrier of 71.3 kcal/mol. The calculated proton abstraction product of **1** with dbu,  $[\text{W}(\text{CO})_5\{\text{Sn}(\text{Ar}^{i\text{Pr}6})\}]^+[\text{H}(\text{dbu})]^-$ , is 18.2 kcal/mol less stable than the observed coordination product **4**.



## INTRODUCTION

Divalent tin(II) hydrides have attracted increasing interest due to their potential catalytic applications in the hydrogenation of unsaturated molecules.<sup>1–9</sup> In 2000, the first stable tin(II) hydride,  $\{\text{Ar}^{i\text{Pr}6}\text{Sn}(\mu\text{-H})\}_2$  ( $\text{Ar}^{i\text{Pr}6} = -\text{C}_6\text{H}_3-2,6-(\text{C}_6\text{H}_2-2,4,6\text{-}i\text{Pr}_3)_2$ ) was reported.<sup>10</sup> This featured a dimeric hydrogen bridged structure. Shortly thereafter, Roesky and co-workers reported the monomeric tin(II) hydrides  $[\{\text{HC}(\text{CMeNAr})_2\}\text{-SnH}]$ <sup>11</sup> and  $[\{\text{ArN}=\text{C}(\text{Me})\}_2\text{C}_6\text{H}_3\text{SnH}]$ <sup>12</sup> ( $\text{Ar} = 2,6\text{-}i\text{Pr}_2\text{C}_6\text{H}_3$ ), which featured terminal Sn–H bonds. Wesemann and co-workers have isolated several three-coordinate monomeric tin(II) hydrides with base-stabilization via reactions of tetravalent organotin trihydrides with Lewis bases.<sup>13–15</sup> Although numerous transition metal-complexed stannylenes<sup>16</sup> compounds and their multiply bonded analogues<sup>17–19</sup> have been reported since the early 1970s, transition metal complexes of hydridostannylenes remain scarce.<sup>20–22</sup> Successful synthetic routes to transition metal-complexed hydridostannylenes include H/Cl exchange as exemplified by the “push–pull” complex,  $\text{IPr}\cdot\text{SnH}_2\cdot\text{W}(\text{CO})_5$ , of Rivard and coworkers.<sup>23</sup> Similar “push–pull” complexes were also reported by Jambor and coworkers with the use of intramolecular base-stabilization.<sup>24</sup> In addition, hydrogen elimination reactions have also been shown to yield transition metal-stabilized hydridostannylenes,  $[\text{Cp}_2\text{Zr}\{\text{Sn}(\text{H})\text{Ar}\}]_2$ .<sup>25,26</sup> In 2021, this group showed that the THF donor ligand in

$[\text{Mo}(\text{CO})_5\text{THF}]$  could be displaced by a hydridostannylene,  $[\text{Ar}^{i\text{Pr}6}\text{SnH}]$ , to give  $\text{Mo}(\text{CO})_5\{\text{Sn}(\text{Ar}^{i\text{Pr}6})\text{H}\}$ .<sup>27</sup> This complex was then shown to effect facile hydrostannylation of  $\text{CO}_2$ , and catalytic hydroboration of  $\text{CO}_2$  was achieved with pinacolborane. These results were in contrast to the lack of catalytic activity for  $\text{CO}_2$  reduction by the parent tin hydride,  $\{\text{Ar}^{i\text{Pr}6}\text{Sn}(\mu\text{-H})\}_2$ .<sup>28</sup>

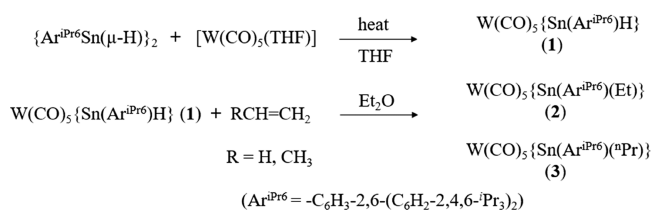
The reactivity of  $\{\text{Ar}^{i\text{Pr}4}\text{Sn}(\mu\text{-H})\}_2$  and  $\{\text{Ar}^{i\text{Pr}6}\text{Sn}(\mu\text{-H})\}_2$  toward olefins has also been investigated, and both  $\{\text{Ar}^{i\text{Pr}4}\text{Sn}(\mu\text{-H})\}_2$  and  $\{\text{Ar}^{i\text{Pr}6}\text{Sn}(\mu\text{-H})\}_2$  were shown to effect facile hydrostannylation of ethylene at room temperature, where the steric properties of the ligands resulted in slightly different reactivity.<sup>29,30</sup> Moreover, it was also discovered that the aryltin(II) hydride  $\{\text{Ar}^{i\text{Pr}4}\text{Sn}(\mu\text{-H})\}_2$  can exist in equilibrium with  $\text{H}_2$  and the distannyne,  $\text{Ar}^{i\text{Pr}4}\text{SnSnAr}^{i\text{Pr}4}$ .<sup>22</sup> Notably, reversible reactions of ethylene with the distannylenes were also reported, where cycloadducts  $\text{Ar}^{i\text{Pr}4}\text{Sn}(\text{CH}_2\text{CH}_2)_2\text{SnAr}^{i\text{Pr}4}$  and  $\text{Ar}^{i\text{Pr}8}\text{Sn}(\text{CH}_2\text{CH}_2)_2\text{SnAr}^{i\text{Pr}8}$  were isolated.<sup>30</sup> Jones and

Received: September 30, 2022

coworkers reported hydrostannylation reactions of  $[\text{LSn}(\mu\text{-H})_2]$  ( $\text{L} = -\text{N}(\text{Ar})(\text{SiPr}^i_3)$ ,  $\text{Ar} = \text{C}_6\text{H}_2\{\text{C}(\text{H})\text{Ph}_2\}_2\text{Pr}^i\text{-2,6,4}$ ) with a variety of alkenes, where the hydrostannylated products suggest equilibrium between the dimer,  $[\text{LSn}(\mu\text{-H})_2]$ , and monomer  $\text{LSnH}$ .<sup>31</sup> However, no catalytic cycle has been achieved in the olefin hydrogenation using tin hydrides despite of the facile reactivity in hydrostannylation of olefins, whereas hydrosilylation reactions of olefins have been reported with silylene supported transition metal complexes.<sup>32,33</sup>

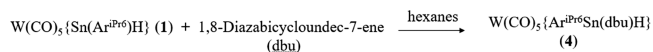
Herein, we report the reactions of  $\{\text{Ar}^{\text{iPr}6}\text{Sn}(\mu\text{-H})_2\}$  with  $[\text{W}(\text{CO})_5(\text{THF})]$ , to give  $\text{W}(\text{CO})_5\{\text{Sn}(\text{Ar}^{\text{iPr}6})\text{H}\}$ , (**1**). Hydrostannylation by **1** of ethylene, or propylene resulted in the formation of  $\text{W}(\text{CO})_5\{\text{Sn}(\text{Ar}^{\text{iPr}6})(\text{Et})\}$ , (**2**), or  $\text{W}(\text{CO})_5\{\text{Sn}(\text{Ar}^{\text{iPr}6})(^n\text{Pr})\}$ , (**3**) (Scheme 1). The Lewis acidic nature of the

### Scheme 1. Syntheses of 1–3



Sn atom in **1** was demonstrated by the formation and isolation of the Lewis acid–base complex  $[(\text{Ar}^{\text{iPr}6})(\text{H})\text{Sn}(\text{dbu})\text{-W}(\text{CO})_5]$ , (**4**), which resulted from the reaction of **1** and the weakly-nucleophilic base,<sup>34</sup> 1,8-diazabicycloundec-7-ene (dbu) (Scheme 2). The catalytic potential of **1** toward ethylene

### Scheme 2. Synthesis of 4



hydrosilylation was also investigated by reacting **2** with  $\text{PhSiH}_3$  in  $\text{C}_6\text{D}_6$ , where limited conversion of **2** to **1** was observed. DFT calculation suggests that the hydrostannylation reactions proceed via olefin insertion into the Sn–H bond by coordination of olefins at the tin atom. The limited conversion in reaction of **2** with  $\text{PhSiH}_3$  in  $\text{C}_6\text{D}_6$  can be accounted for in terms of the rate-determining step in the metathesis reaction between Sn–C/Si–H bond having a very high energy barrier of 71.3 kcal/mol.

## EXPERIMENTAL SECTION

**General Considerations.** All operations were carried out by using modified Schlenk techniques or in a Vacuum Atmospheres OMNI-Lab drybox under an atmosphere of dry argon or nitrogen. All solvents were dried over alumina columns and degassed prior to use.<sup>35</sup> The metal carbonyls were used as purchased without further purification.  $^1\text{H}$ ,  $^{13}\text{C}\{^1\text{H}\}$ ,  $^{29}\text{Si}\{^1\text{H}\}$ , and  $^{119}\text{Sn}\{^1\text{H}\}$  NMR spectra were collected on a Bruker 400 MHz Nanobay Avance III HD spectrometer. The  $^{119}\text{Sn}$  NMR data were referenced to the external standard  $\text{SnMe}_4$ . UV–visible spectra were recorded in dilute hexane solutions in 3.5 mL quartz cuvettes using an Olis 17 Modernized Cary 14 UV–Vis/NIR spectrophotometer. Infrared spectra were collected on a Bruker Tensor 27 ATR-FTIR spectrometer.  $\{\text{Ar}^{\text{iPr}6}\text{Sn}(\mu\text{-H})_2\}$ <sup>10</sup> and  $[\text{W}(\text{CO})_5(\text{THF})]$ <sup>36</sup> were synthesized by the literature methods. All synthesized compounds hydrolyzed rapidly in air, and therefore no elemental analysis was carried out.

**Syntheses.**  $\text{W}(\text{CO})_5\{\text{Sn}(\text{Ar}^{\text{iPr}6})\text{H}\}$  (**1**). A solution of  $[\text{W}(\text{CO})_5(\text{THF})]$  (1.40 mmol, from 0.352 g  $\text{W}(\text{CO})_6$ ) in THF (ca. 40 mL) was added to a heavy-walled Teflon tapped Schlenk flask along with  $\{\text{Ar}^{\text{iPr}6}\text{SnH}\}_2$  (0.705 g, 0.586 mmol) in THF (ca. 30 mL).

Upon addition of  $[\text{W}(\text{CO})_5(\text{THF})]$ , the color of the solution changed from blue to green, and then to a yellow orange color after heating at 50 °C for 1 day, after which the reaction mixture was heated for 2 additional days. The solution was then cooled to room temperature; the solvent was removed under reduced pressure, and the residue was extracted with ca. 50 mL of hexanes and filtered. Storage of the solution in a ca. –30 °C freezer for 2 weeks afforded crystals as pale yellow blocks that proved suitable for single crystal X-ray studies. Yield: 75.3% (0.817 g, 0.882 mmol).  $^1\text{H}$  NMR ( $\text{C}_6\text{D}_6$ , 399.8 MHz, 298 K):  $\delta$  1.06 (d, 12 H,  $J_{\text{HH}} = 6.7$  Hz,  $o\text{-CH}(\text{CH}_3)_2$ ), 1.22 (d, 12 H,  $J_{\text{HH}} = 7.2$  Hz,  $o\text{-CH}(\text{CH}_3)_2$ ), 1.40 (d, 12 H,  $J_{\text{HH}} = 7.0$  Hz,  $p\text{-CH}(\text{CH}_3)_2$ ), 2.77 (sept, 2 H,  $J_{\text{HH}} = 6.8$  Hz,  $p\text{-CH}(\text{CH}_3)_2$ ), 3.09 (sept, 4 H,  $J_{\text{HH}} = 6.9$  Hz,  $o\text{-CH}(\text{CH}_3)_2$ ), 7.19 (s, 4 H,  $m\text{-C}_6\text{H}_2$ ), 7.28 (s, 3 H,  $m\text{-C}_6\text{H}_3$  and  $p\text{-C}_6\text{H}_3$ ), 18.62 (s, 1 H,  $J_{\text{W-H}} = 19$  Hz,  $J_{\text{Sn-H}} = 754$  Hz,  $\text{Sn-H}$ );  $^{13}\text{C}\{^1\text{H}\}$  NMR ( $\text{C}_6\text{D}_6$ , 100.5 MHz, 298 K):  $\delta$  23.39, 23.97, 26.28, 31.15, 34.76, 122.66, 128.83, 129.99, 133.61, 145.21, 150.72, 161.20, 196.80 ( $J_{\text{W-C}} = 121$  Hz), 201.28;  $^{119}\text{Sn}\{^1\text{H}\}$  NMR ( $\text{C}_6\text{D}_6$ , 149.3 MHz, 298 K):  $\delta$  1159 (d,  $J_{\text{Sn-W}} = 674$  Hz).  $\lambda_{\text{max}}$  ( $\epsilon$ ): 397 nm ( $5.5 \times 10^3$  L mol<sup>–1</sup> cm<sup>–1</sup>). IR ( $\nu$ , cm<sup>–1</sup>): 2066 (m), 1915 (vs), 1757 (w).

$\text{W}(\text{CO})_5\{\text{Sn}(\text{Ar}^{\text{iPr}6})(\text{Et})\}$  (**2**). A solution of **1** (0.381 g, 0.410 mmol) in  $\text{Et}_2\text{O}$  (ca. 40 mL) was added to a heavy-walled Teflon tapped Schlenk flask. The flask was frozen by immersion in liquid nitrogen, evacuated under reduced pressure, and refilled with ethylene at room temperature, whereupon the reaction was stirred at room temperature for additional 15 min. The solvent was concentrated under reduced pressure to ca. 5 mL. Storage of the solution in a ca. –30 °C freezer for 1 week afforded yellow-orange blocks that were suitable for single crystal X-ray diffraction studies. Yield: 27.2% (0.107 g, 0.111 mmol).  $^1\text{H}$  NMR ( $\text{C}_6\text{D}_6$ , 399.8 MHz, 298 K):  $\delta$  0.89–1.09 (m, 5 H,  $\text{Sn-CH}_2\text{CH}_3$ ), 1.06 (d, 12 H,  $J_{\text{HH}} = 6.7$  Hz,  $o\text{-CH}(\text{CH}_3)_2$ ), 1.21 (d, 12 H,  $J_{\text{HH}} = 6.3$  Hz,  $o\text{-CH}(\text{CH}_3)_2$ ), 1.37 (d, 12 H,  $J_{\text{HH}} = 6.3$  Hz,  $p\text{-CH}(\text{CH}_3)_2$ ), 2.76 (sept, 2 H,  $J_{\text{HH}} = 7.0$  Hz,  $p\text{-CH}(\text{CH}_3)_2$ ), 3.11 (br, 4 H,  $o\text{-CH}(\text{CH}_3)_2$ ), 7.19 (s, 4 H,  $m\text{-C}_6\text{H}_2$ ), 7.28–7.33 (m, 3 H,  $m\text{-C}_6\text{H}_3$  and  $p\text{-C}_6\text{H}_3$ );  $^{13}\text{C}\{^1\text{H}\}$  NMR ( $\text{C}_6\text{D}_6$ , 100.5 MHz, 298 K):  $\delta$  8.66, 22.73, 23.93, 26.89, 30.98, 34.80, 40.49, 122.45, 128.41, 131.05, 135.48, 144.56, 147.13, 150.29, 165.41, 197.82, 201.47;  $^{119}\text{Sn}\{^1\text{H}\}$  NMR ( $\text{C}_6\text{D}_6$ , 149.3 MHz, 298 K):  $\delta$  1455.  $\lambda_{\text{max}}$  ( $\epsilon$ ): 311 nm (shoulder,  $4.6 \times 10^3$  L mol<sup>–1</sup> cm<sup>–1</sup>), 394 nm ( $4.4 \times 10^3$  L mol<sup>–1</sup> cm<sup>–1</sup>). IR ( $\nu$ , cm<sup>–1</sup>): 2059 (m), 1920 (vs).

$\text{W}(\text{CO})_5\{\text{Sn}(\text{Ar}^{\text{iPr}6})(^n\text{Pr})\}$  (**3**). A procedure similar to that used for the preparation of **2** was carried out using propylene, and 0.269 g and 0.291 mmol of **1**. Storage of the solution in a ca. –30 °C freezer for 1 week afforded yellow needle crystals. Yield: 30.2% (0.085 g, 0.088 mmol).  $^1\text{H}$  NMR ( $\text{C}_6\text{D}_6$ , 399.8 MHz, 298 K):  $\delta$  0.80–0.91 (m, 2 H,  $\text{Sn-CH}_2\text{CH}_2\text{CH}_3$ ), 0.99 (t, 2 H,  $J_{\text{HH}} = 7.1$  Hz,  $\text{Sn-CH}_2\text{CH}_2\text{CH}_3$ ), 1.07 (d, 12 H,  $J_{\text{HH}} = 6.7$  Hz,  $o\text{-CH}(\text{CH}_3)_2$ ), 1.22 (d, 12 H,  $J_{\text{HH}} = 7.1$  Hz,  $o\text{-CH}(\text{CH}_3)_2$ ), 1.23–1.29 (m, 3 H,  $\text{Sn-CH}_2\text{CH}_2\text{CH}_3$ ), 1.39 (d, 12 H,  $J_{\text{HH}} = 6.7$  Hz,  $p\text{-CH}(\text{CH}_3)_2$ ), 2.77 (sept, 2 H,  $J_{\text{HH}} = 7.1$  Hz,  $p\text{-CH}(\text{CH}_3)_2$ ), 3.13 (br, 4 H,  $o\text{-CH}(\text{CH}_3)_2$ ), 7.19 (s, 4 H,  $m\text{-C}_6\text{H}_2$ ), 7.24–7.34 (m, 3 H,  $m\text{-C}_6\text{H}_3$  and  $p\text{-C}_6\text{H}_3$ );  $^{13}\text{C}\{^1\text{H}\}$  NMR ( $\text{C}_6\text{D}_6$ , 100.5 MHz, 298 K):  $\delta$  18.75, 19.04, 22.75, 23.96, 26.92, 30.93, 34.80, 51.13, 122.45, 128.41, 131.05, 135.68, 144.64, 147.09, 150.27, 165.32, 197.96 ( $J_{\text{W-C}} = 121$  Hz), 201.54;  $^{119}\text{Sn}\{^1\text{H}\}$  NMR ( $\text{C}_6\text{D}_6$ , 149.3 MHz, 298 K):  $\delta$  1443.  $\lambda_{\text{max}}$  ( $\epsilon$ ): 307 nm (shoulder,  $6.5 \times 10^3$  L mol<sup>–1</sup> cm<sup>–1</sup>), 394 nm ( $6.3 \times 10^3$  L mol<sup>–1</sup> cm<sup>–1</sup>). IR ( $\nu$ , cm<sup>–1</sup>): 2059 (m), 1920 (vs).

$\text{W}(\text{CO})_5\{\text{Sn}(\text{Ar}^{\text{iPr}6})(\text{dbu})\text{H}\}$  (**4**). To a Schlenk flask charged with **1** (0.259 g, 0.280 mmol) and dbu (44  $\mu\text{L}$ , 0.295 mmol), ca. 50 mL of hexanes were added. Upon addition of solvent, the color of the solution lightened from yellow-orange to pale yellow. Then, the solution was stirred overnight and concentrated under reduced pressure to ca. 10 mL. Storage of the solution in a ca. –30 °C freezer for 2 weeks afforded colorless blocks that were suitable for single crystal X-ray studies. Yield: 46.4% (0.141 g, 0.130 mmol).  $^1\text{H}$  NMR ( $\text{C}_6\text{D}_6$ , 399.8 MHz, 298 K):  $\delta$  0.70–0.99 (m, 4 H, dbu), 1.15 (d, 12 H,  $J_{\text{HH}} = 6.7$  Hz,  $o\text{-CH}(\text{CH}_3)_2$ ), 1.19–1.24 (m, 3 H, dbu), 1.29 (d, 12 H,  $J_{\text{HH}} = 6.7$  Hz,  $o\text{-CH}(\text{CH}_3)_2$ ), 1.33 (d, 6 H,  $J_{\text{HH}} = 6.6$  Hz,  $p\text{-CH}(\text{CH}_3)_2$ ), 1.38–1.54 (m, 2 H, dbu), 1.59 (d, 6 H,  $J_{\text{HH}} = 6.7$  Hz,  $p\text{-CH}(\text{CH}_3)_2$ ), 1.99–2.14 (m, 2 H, dbu), 2.23–2.38 (m, 2 H, dbu),

2.63–2.76 (m, 1 H, dbu), 2.89 (sept., 2 H,  $J_{\text{HH}} = 6.9$  Hz,  $o\text{-CH}(\text{CH}_3)_2$  and 1 H, dbu), 2.97 (sept., 2 H,  $J_{\text{HH}} = 6.6$  Hz,  $o\text{-CH}(\text{CH}_3)_2$ ), 3.02–3.12 (m, 1 H, dbu), 3.32 (sept., 2 H,  $J_{\text{HH}} = 6.6$  Hz,  $p\text{-CH}(\text{CH}_3)_2$ ), 7.08–7.14 (m, 3 H,  $m\text{-C}_6\text{H}_3$  and  $p\text{-C}_6\text{H}_3$ ), 7.20 (s, 2 H,  $m\text{-C}_6\text{H}_2$ ), 7.26 (s, 2 H,  $m\text{-C}_6\text{H}_2$ ), 10.12 (s, 1 H,  $J_{\text{W-H}} = 19$  Hz,  $J_{\text{Sn-H}}^{119} = 1093$  Hz,  $J_{\text{Sn-H}}^{117} = 1045$  Hz,  $J_{\text{W-H}} = 12$  Hz, Sn–H);  $^{13}\text{C}\{^1\text{H}\}$  NMR ( $\text{C}_6\text{D}_6$ , 100.5 MHz, 298 K):  $\delta$  23.47, 23.61, 23.84, 24.31, 24.60, 26.01, 26.31, 26.58, 30.98, 31.42, 34.98, 48.44, 53.10, 121.46, 126.20, 131.86, 140.11, 146.99, 147.63, 148.67, 150.35, 167.51, 201.95, 202.77;  $^{119}\text{Sn}\{^1\text{H}\}$  NMR ( $\text{C}_6\text{D}_6$ , 149.3 MHz, 298 K):  $\delta$  not detected.  $\lambda_{\text{max}}$  ( $\epsilon$ ): 357 nm (shoulder,  $2.4 \times 10^3$  L mol $^{-1}$  cm $^{-1}$ ). IR ( $\nu$ , cm $^{-1}$ ): 2050 (m), 1963 (m), 1916 (s), 1887 (vs), 1793 (w), 1575 (m).

**Catalytic Studies.** To a J. Young's tube containing ca. 0.02 g of **2**, was added 0.6 mL of  $\text{C}_6\text{D}_6$ , then an excess amount of  $\text{PhSiH}_3$  was added to the tube. The reactions were monitored by  $^1\text{H}$  and  $^{29}\text{Si}$  NMR spectroscopies, and  $^1\text{H}$  and  $^{29}\text{Si}$  NMR spectra were recorded after a brief sonication of the mixture. Additional  $^1\text{H}$  NMR spectra of the mixture of **2** and  $\text{PhSiH}_3$  in  $\text{C}_6\text{D}_6$  were taken 12, 24, and 72 h after mixing in glove box, separately. No color change was observed upon addition of  $\text{PhSiH}_3$  to the  $\text{C}_6\text{D}_6$  solution of **2**; however, a minor color change from bright yellow to yellow-orange was observed upon heating mixture solution at ca. 65 °C after ca. 60 h (see SI).

## RESULTS AND DISCUSSION

**Syntheses.** Compound **1** was synthesized by a similar procedure to that described in a previous publication;<sup>27</sup> it was obtained by gently heating 1 equivalent of THF solution of  $\{\text{Ar}^{\text{iPr6}}\text{Sn}(\mu\text{-H})\}_2$ <sup>10</sup> with 2 equivalents of  $[\text{W}(\text{CO})_5(\text{THF})]$ ,<sup>36</sup> and isolated with good yield, 75.3%. (Scheme 1) Alternatively, Jambor and coworkers demonstrated that transition metal complexed hydridostannylene can be synthesized via halide elimination reaction of  $\text{L}^2(\text{Cl})\text{Sn-W}(\text{CO})_5$  ( $\text{L}^2 = 2\text{-Et}_2\text{NCH}_2\text{-4,6-}t\text{Bu}_2\text{-C}_6\text{H}_2$ ) with  $\text{KEt}_3\text{BH}$ .<sup>24</sup> However, this synthetic route is inapplicable for terphenyl ligand supported species as shown previously. The oxidative addition of organolead(II) bromide with  $[\text{W}(\text{CO})_5\text{THF}]$  forms a bridged plumblyne complex instead of formation of a plumblyne coordination transition metal complex.<sup>37</sup> Wesemann and coworkers have also successfully isolated transition metal complexed hydridostannylene via different synthetic routes, such as  $\text{H}_2$  elimination from an organotin trihydride,<sup>26</sup> or reaction of a low valent aryl tin cation with transition metal hydrides.<sup>25</sup> For the synthesis of **2** and **3** (Scheme 1), a solution of **1** in  $\text{Et}_2\text{O}$  was frozen, and the flask was evacuated under reduced pressure. The reaction flask was then allowed to warm to room temperature, and refilled with ethylene, or propylene, whereupon the color of the solution changed from yellow-orange to bright yellow. Stirring of the resultant solution for 30 min afforded a quantitative conversion based on the  $^1\text{H}$  NMR spectrum of the crude solution mixture. Concentration of the solution, followed by storage in a ca. –30 °C freezer for 1 week, afforded yellow crystals of **2** or **3** in moderate yield. Jones and coworkers have also reported the facile hydrostannylation reactions of unactivated alkenes with  $[\text{LSn}(\mu\text{-H})_2]$  ( $\text{L} = \text{N}(\text{Ar})(\text{SiPr}^i_3)$ ,  $\text{Ar} = \text{C}_6\text{H}_2\{\text{C}(\text{H})\text{Ph}\}_2\text{Pr}^i\text{-2,6,4}$ ) at low temperature (ca. –80 °C) due to the mild thermal instability of the tin hydride species at room temperature, nevertheless these products were isolated with good yields.<sup>38</sup> Wesemann and co-workers reported hydrostannylation of styrene at slightly elevated temperature (ca. 75 °C) with  $[\text{Cp}_2\text{W}(\text{H})=\text{SnHAr}^{\text{iPr6}}]^+$  to afford  $[\text{Cp}_2\text{W}(\text{H})\text{Sn}(\text{CH}_2\text{CH}_2\text{Ph})\text{Ar}^{\text{iPr6}}]^+$  possibly due to the increased steric bulk from the phenyl group of styrene.<sup>25</sup>

Initial attempts to add dbu, a known weakly nucleophilic base,<sup>34</sup> to a solution of **1** was for the purpose of  $\text{pK}_a$  determination of the complex reported in previous work of

this group.<sup>27</sup> However, the  $^1\text{H}$  NMR spectrum of the crude product showed quantitative coordination reaction rather than a Brønsted–Lowry acid–base reaction between the tin hydride species and dbu. Compound **4** was synthesized by addition of slight excess of dbu (1.05 equivalents) into a solution of **1** in hexanes at room temperature. The mixture was stirred overnight, whereupon the color of the solution changed from yellow-orange to very pale yellow. Concentration of the resultant solution followed by storage in a ca. –30 °C freezer for 2 weeks afforded colorless crystals of **4** in moderate yield.

**Structures.** The molecular structures of **1**, **2**, and **4** are shown in Figures 1, 2, and 3, respectively.

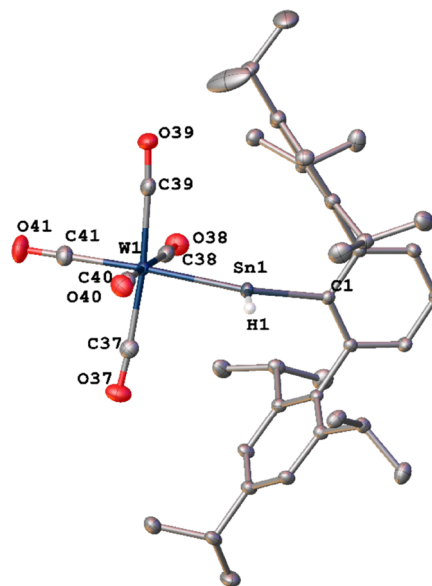


**Figure 1.** Solid-state molecular structure of **1** (hydrogen atoms, except for tin bound H1, and ligand disorder are not shown for clarity). Thermal ellipsoids are shown at 30% probability. Selected bond lengths (Å) and angles (degrees): Sn(1)–C(1) 2.1518(19), Sn(1)–W(1) 2.7150(2), Sn(1)–H(1) 2.06(3), W(1)–C(37) 2.051(2), W(1)–C(38) 2.049(2), W(1)–C(39) 2.047(2), W(1)–C(40) 2.041(2), W(1)–C(41) 2.006(2), C(37)–O(37) 1.138(3), C(38)–O(38) 1.136(3), C(39)–O(39) 1.140(3), C(40)–O(40) 1.143(3), C(41)–O(41) 1.137(3); C(1)–Sn(1)–W(1) 141.34 (5), C(1)–Sn(1)–H(1) 107.9(7), W(1)–Sn(1)–H(1) 110.7(7).

The molecular structure of **1** shows that the tin atom is three-coordinate and is bound to the  $\text{Ar}^{\text{iPr6}}$  ligand via C(1), a hydrogen atom, and a  $[\text{W}(\text{CO})_5]$  fragment. Compound **1** displays similar structural features to those of  $\text{Mo}(\text{CO})_5\{\text{Sn}(\text{Ar}^{\text{iPr6}})\text{H}\}$ <sup>27</sup> reported earlier by this group, where the hydridostannylene,  $[\text{Ar}^{\text{iPr6}}\text{SnH}]$ , forms Lewis acid–base complex with  $[\text{W}(\text{CO})_5]$  to afford almost planar coordination geometry at the tin atom, and distorted octahedral geometry at the tungsten atom, respectively. The sum of C(1)–Sn(1)–W(1), C(1)–Sn(1)–H(1), and W(1)–Sn(1)–H(1) angles around tin in complex **1** is 359.9(7)°. The almost planar coordination geometry at Sn that is imposed by the ligands agrees with the presence of a vacant p orbital oriented perpendicular to the coordination plane in the structure of **1**, which can be further demonstrated in the DFT calculations of optimized structure of **1** in gas phase (see ESI). In the structure of **1**, the C(1)–Sn(1)–H(1) unit is almost coplanar with that of tungsten and the three carbonyl groups of C(38), C(40), and C(41). The Sn(1)–W(1)–C(41) array is almost



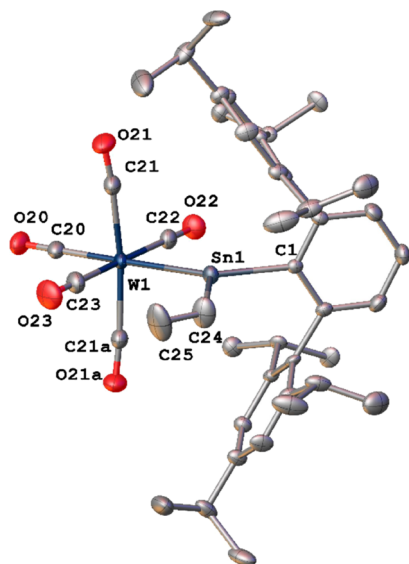


**Figure 2.** Solid-state molecular structure of **2** (hydrogen atoms and ligand disorder are not shown for clarity). Thermal ellipsoids are shown at 30% probability. Selected bond lengths (Å) and angles (degrees): Sn(1)–C(1) 2.166(3), Sn(1)–W(1) 2.7286(3), Sn(1)–C(24) 2.180(6), W(1)–C(20) 2.007(4), W(1)–C(21) 2.042(3), W(1)–C(22) 2.061(5), W(1)–C(23) 2.023(5), C(20)–O(20) 1.146(5), C(21)–O(21) 1.143(4), C(22)–O(22) 1.131(5), C(23)–O(23) 1.145(5), C(24)–C(25) 1.42(2), C(1)–Sn(1)–W(1) 135.13(8), C(1)–Sn(1)–C(24) 105.68(19), W(1)–Sn(1)–C(24) 118.68(18).

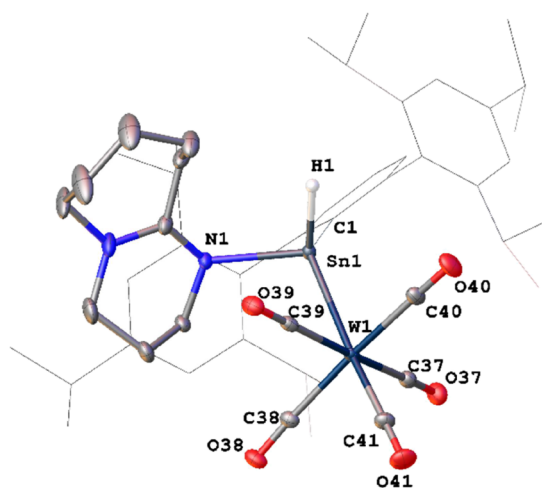


**Figure 3.** Solid-state molecular structure of **4** (Ar<sup>iPr6</sup> substituent is shown as wireframe, and hydrogen atoms except for the tin bound H1, and ligand disorder are not shown for clarity). Thermal ellipsoids are shown at 30% probability. Selected bond lengths (Å) and angles (degrees): Sn(1)–C(1) 2.2031(18), Sn(1)–N(1) 2.2261(16), Sn(1)–W(1) 2.8063(2), Sn(1)–H(1) 1.68(3), W(1)–C(37) 2.046(2), W(1)–C(38) 2.023(3), W(1)–C(39) 2.024(2), W(1)–C(40) 2.043(2), W(1)–C(41) 1.983(2), C(37)–O(37) 1.142(3), C(38)–O(38) 1.147(3), C(39)–O(39) 1.148(3), C(40)–O(40) 1.141(3), C(41)–O(41) 1.155(3); C(1)–Sn(1)–W(1) 131.31(5), C(1)–Sn(1)–H(1) 101.6(9), C(1)–Sn(1)–N(1) 105.21(7), W(1)–Sn(1)–H(1) 111.7(9).

linear (176.23(7)°). The coordination reaction of dbu with compound **1** affords compound **4**. The molecular structure of **4** features Lewis acid–base complex with a four-coordinate tin atom to which dbu is also coordinated. This structure of **4**

represents the first structurally characterized Sn–dbu coordination species. The Lewis acid–base reaction is likely to proceed via coordination of dbu to the vacant p orbital at the tin atom, located perpendicular to the tin coordination plane in the structure of **1**. However, the Sn(1)–N(1) bond vector in the structure of **4** is not perpendicular to the coordination plane, as shown by the bond angles of N(1)–Sn(1)–H(1), 96.5(9)°; N(1)–Sn(1)–C(1), 105.21(7)°; and N(1)–Sn(1)–W(1), 105.12(5)°. The sum of the angles at tin associated with the hydride and terphenyl ligand in **4**, C(1)–Sn(1)–H(1), C(1)–Sn(1)–W(1), and W(1)–Sn(1)–H(1), is 344.6(9)°. The Sn(1)–N(1) distance is 2.2261(16) Å in **4**, which is slightly longer than the sum of covalent radii of Sn (1.40 Å) and N (0.71 Å).<sup>39</sup> The Sn(1)–N(1) distance in **4** is in close agreement with that in the four-coordinate transition metal complexed hydridostannylene, (Sn–N 2.292(3) Å) in L<sup>2</sup>(H)SnW(CO)<sub>5</sub> (L<sup>2</sup> = 2-Et<sub>2</sub>NCH<sub>2</sub>-4,6-*t*Bu<sub>2</sub>-C<sub>6</sub>H<sub>2</sub>), which was reported by Jambor and co-workers.<sup>24</sup> The Sn(1)–N(1) distance in **4** is also similar to [HC(CMeNAr)<sub>2</sub>]SnH (Ar = 2,6-*i*Pr<sub>2</sub>C<sub>6</sub>H<sub>3</sub>), reported by Roesky and co-workers.<sup>11</sup> In comparison to Sn–N distances of bis(amido)stannylene, such as Sn{N(SiMe<sub>3</sub>)<sub>2</sub>}<sub>2</sub><sup>40</sup> and of *N*-heterocyclic stannylenes,<sup>41,42</sup> **4** displays a longer Sn–N distance likely due to the dative N → Sn bond coordination. Other examples of Sn–N dative bond coordination include [2,6-(Me<sub>2</sub>-NCH<sub>2</sub>)<sub>2</sub>C<sub>6</sub>H<sub>3</sub>(Cl)SnW(CO)<sub>5</sub>], reported by Jurkschat and co-workers, with Sn–N distances of 2.543(3) and 2.5526(3) Å, and shortening to 2.264(2) Å upon displacing chloride with aqua-coordination in [2,6-(Me<sub>2</sub>-NCH<sub>2</sub>)<sub>2</sub>C<sub>6</sub>H<sub>3</sub>(H<sub>2</sub>O)SnW(CO)<sub>5</sub>]<sup>+</sup>[CB<sub>11</sub>H<sub>12</sub>]<sup>−</sup>.<sup>43</sup> The positions of the hydrogen atoms bound to the tin atoms in both **1** and **4** were located in the Fourier difference map and refined isotropically. The Sn–H distance is 2.09 Å in **1**, may be compared to the Sn–H distance 1.93(2) Å in the previously reported Mo(CO)<sub>5</sub>{Sn(Ar<sup>iPr6</sup>)-H}.<sup>27</sup> The Sn–H distance is 1.68(3) Å in **4**, which is similar to the Sn–H, 1.82(6) Å, in Mo(CO)<sub>5</sub>{Sn(Ar<sup>iPr4</sup>)(THF)H}.<sup>27</sup> These values may be compared to that of the terminal Sn–H bond, 1.74(3) Å in [HC(CMeNAr)<sub>2</sub>]SnH<sup>11</sup> reported by Roesky and co-workers, 1.797(2) Å in L<sup>2</sup>(Cl)Sn–W(CO)<sub>5</sub>,<sup>24</sup> reported by Jambor and co-workers, 1.81(11) Å in IPr–SnH<sub>2</sub>–W(CO)<sub>5</sub>,<sup>23</sup> reported by Rivard and co-workers, and Sn–H bonds in Cp<sub>2</sub>M(Ar<sup>iPr6</sup>SnH)<sub>2</sub> (M = Ti, Zr, and Hf)<sup>26</sup> complexes reported by Wesemann and co-workers, which range from 1.69(2) to 1.776(18) Å.

Insertion of ethylene, or propylene, into the Sn–H bond in **1** yielded compound **2** or **3**, respectively. The molecular structure of **2** shows little variation from the structure of **1**, as the tin atom in **2** remains three-coordinate. The Sn–C(alkyl) distance in **2** is 2.180(6) Å. This distance is comparable to the literature Sn–alkyl distances which range from 2.145(7) to 2.187(8) Å.<sup>29,38</sup> The sum of the angles around tin is 359.5(2)°. The structure of **2** also displays coplanar coordination to the metal carbonyl fragment, where the C(1)–Sn(1)–alkyl unit is almost coplanar with that of tungsten and the three carbonyl groups. The Sn(1)–W(1) bond is almost co-linear with the carbonyl group C(20)–O(20) in *trans* position to the stannylene, 178.07(12)°.

In the structures of **1**, **2**, and **4**, the average W–CO bond lengths of four carbonyls that are in *cis* positions relative to the stannylene ligand are slightly longer than those of the *trans*-positioned carbonyl group, suggesting a stronger  $\pi$ -backbonding for the *trans* W–CO bond. However, in the structure of **4**, the average bond length of W–CO for the four carbonyls

that are in *cis* positions to the stannylene are slightly shortened to 2.034(3) Å, and the *trans* W–CO bond is shortened to 1.983(2) Å when compared to *trans* W–CO bonds in **1** and **2**. In turn, these bonds are comparable to the *trans* W–CO bond shortening with THF coordination in Mo(CO)<sub>5</sub>{Sn(Ar<sup>iPr6</sup>)(THF)H}.<sup>27</sup> This is likely a result of the increased electron density at tungsten due to the coordination of dbu and disrupting of  $\pi$ -backbonding between the hydridostannylene and W(CO)<sub>5</sub>, and therefore stronger  $\pi$ -backbonding between the tungsten atom and the *trans* carbonyl group. The Sn–W distances for **1**, **2**, and **4** range from 2.7150(2) to 2.8063(2) Å. These values are in close agreement with the sum of the covalent radii of Sn (1.40 Å) and W (1.37 Å).<sup>39</sup> The Sn–W distances are comparable to the reported singly bonded stannylene–W(CO)<sub>5</sub> complexes.<sup>24,43–47</sup> The Sn=W double bond in [Cp<sub>2</sub>W(H)=SnHAr<sup>iPr6</sup>]<sup>+</sup> was reported to be 2.6221(2) Å by Wesemann and co-workers,<sup>25</sup> in comparison to the Sn–W triple bonds<sup>48</sup> in stannylene complexes, such as *trans*-[Cl(dppe)<sub>2</sub>W≡Sn–C<sub>6</sub>H<sub>3</sub>-2,6-Mes<sub>2</sub>] and [(dppe)<sub>2</sub>W≡Sn–C<sub>6</sub>H<sub>3</sub>-2,6-Mes<sub>2</sub>]<sup>+</sup>[PF<sub>6</sub>]<sup>–</sup> (dppe = Ph<sub>2</sub>PCH<sub>2</sub>CH<sub>2</sub>PPh<sub>2</sub>, Mes = C<sub>6</sub>H<sub>2</sub>-2,4,6-Me<sub>3</sub>) that were reported by Filippou and co-workers.<sup>17,18</sup> Nonetheless, the Sn–W distances reported here are shorter than those of metallostannylene complexes of tungsten such as [Cp\*<sup>+</sup>(CO)<sub>3</sub>W–SnCl(Idipp)]<sup>+</sup> (2.9514(4) Å) (Idipp = C[N(C<sub>6</sub>H<sub>3</sub>-2,6-<sup>i</sup>Pr<sub>2</sub>)CH]<sub>2</sub>) reported by Filippou and coworkers, or Ar<sup>Me6</sup>Sn–WCp(CO)<sub>3</sub> (2.9107(10) Å) (Ar<sup>Me6</sup> = –C<sub>6</sub>H<sub>3</sub>-2,6-(C<sub>6</sub>H<sub>2</sub>-2,4,6-Me<sub>3</sub>)<sub>2</sub>) and Ar<sup>iPr6</sup>Sn–WCp(CO)<sub>3</sub> (2.9030(8) Å) reported by this group.<sup>50,51</sup>

**NMR Spectroscopy.** All <sup>1</sup>H, <sup>13</sup>C{<sup>1</sup>H}, and <sup>119</sup>Sn{<sup>1</sup>H} NMR spectroscopic data are listed in greater detail in the Supporting Information. The solution <sup>1</sup>H NMR spectra of **1–4** displayed signals corresponding to the Ar<sup>iPr6</sup> ligands with diastereotopic isopropyl methyl groups and septet methine proton signals and showed small changes with respect to those reported for Mo(CO)<sub>5</sub>{Sn(Ar<sup>iPr6</sup>)H}<sup>27</sup> or {Ar<sup>iPr6</sup>Sn( $\mu$ -H)}<sub>2</sub>.<sup>10</sup> The Sn–H signal for **1** was observed at  $\delta$  = 18.62 ppm. This is flanked by the <sup>117/119</sup>Sn satellites <sup>1</sup>J<sub>Sn–H</sub> = 754 Hz, and coupling to tungsten <sup>183</sup>W, <sup>2</sup>J<sub>W–H</sub> = 19 Hz, which is consistent with the Sn–H signal observed in the <sup>1</sup>H NMR spectrum of Mo(CO)<sub>5</sub>{Sn(Ar<sup>iPr6</sup>)H},  $\delta$  = 18.00 ppm.<sup>27</sup> The chemical shift of the Sn–H signal and the observed coupling constant of **1** are in close agreement with the reported values for tantalum and tungsten coordinated hydridostannylenes, [Cp<sub>2</sub>W(H)=SnHAr<sup>iPr6</sup>]<sup>+</sup>[Al(OC{CF<sub>3</sub>})<sub>3</sub>]<sub>4</sub>,  $\delta$  = 15.13 ppm, <sup>1</sup>J<sub>Sn–H</sub> = 1040 Hz, and <sup>2</sup>J<sub>W–H</sub> = 32 Hz, and [Cp<sub>2</sub>TaH<sub>2</sub>–SnHAr<sup>iPr6</sup>]<sup>+</sup>[Al(OC{CF<sub>3</sub>})<sub>3</sub>]<sub>4</sub>,  $\delta$  = 15.55 ppm, and <sup>1</sup>J<sub>Sn–H</sub> = 1165 Hz.<sup>25</sup> The Sn–H signal for **4** was observed at  $\delta$  = 10.12 ppm, flanked by the respective <sup>117/119</sup>Sn satellites <sup>1</sup>J<sup>119</sup><sub>Sn–H</sub> = 1093 Hz, <sup>1</sup>J<sup>117</sup><sub>Sn–H</sub> = 1045 Hz, and <sup>183</sup>W <sup>2</sup>J<sub>W–H</sub> = 12 Hz, which is much further upfield than the Sn–H signals for **1**, Mo(CO)<sub>5</sub>{Sn(Ar<sup>iPr6</sup>)H}, and  $\delta$  = 17.09 ppm for Mo(CO)<sub>5</sub>{Sn(Ar<sup>iPr4</sup>)(THF)H}.<sup>27</sup> Relevant species also includes the hydridostannylene complex, Cp\*<sup>+</sup>(<sup>i</sup>Pr<sub>3</sub>P)(H)Os=SnH(trip) (trip = 2,4,6-triisopropylphenyl) with a resonance at  $\delta$  = 19.4 ppm, by Tilley and co-workers.<sup>52</sup> Compared to **1**, the upfield shift of the Sn–H signal in **4** can be attributed to the increased electron density at the tin atom due to dbu coordination at the tin atom, and that dbu is a better  $\sigma$ -donor than THF. The calculated <sup>1</sup>H NMR chemical shift of the Sn–H hydrogen of the hypothetical monomeric unit of {Ar<sup>iPr6</sup>Sn( $\mu$ -H)}<sub>2</sub> is  $\delta$  = 25.4 ppm,<sup>53</sup> and the reported chemical shifts of *N*-heterocyclic carbene (NHC) coordinated three-coordinate hydridostannylenes range from  $\delta$  = 6.91 to  $\delta$  = 7.23 ppm, with <sup>1</sup>J<sub>Sn–H</sub> coupling constants of 192

to 237 Hz.<sup>14,15</sup> In comparison to these NHC-coordinated hydridostannylenes, the Sn–H chemical shift of **4** can be explained by reduced electron density at the tin atom which should result in a downfield shift due to coordination of transition metal carbonyl moiety.<sup>16</sup> The chemical shift of Sn–H signal and coupling constant of **4** is comparable to the reported values for L<sup>2</sup>(H)Sn–W(CO)<sub>5</sub> (L<sup>2</sup> = 2-Et<sub>2</sub>NCH<sub>2</sub>-4,6-*t*Bu<sub>2</sub>-C<sub>6</sub>H<sub>2</sub>),  $\delta$  = 10.25 ppm, <sup>1</sup>J<sub>Sn–H</sub> = 1091 Hz, and <sup>1</sup>J<sub>W–H</sub> = 15.6 Hz, reported by Jambor and co-workers.<sup>24</sup> Diffusion-ordered spectroscopy (DOSY) <sup>1</sup>H NMR spectroscopy of **4** afforded a diffusion coefficient of 4.42 × 10<sup>–10</sup> m<sup>2</sup>/s, which suggested that no dissociation of the dbu molecule occurred in the C<sub>6</sub>D<sub>6</sub> solution of **4**. The <sup>1</sup>H NMR spectrum of **2** showed broad resonances at  $\delta$  = 0.89–1.09 ppm for the corresponding ethyl group, which agrees with the shifts from the ethyl group in the <sup>1</sup>H NMR spectrum of {Ar<sup>iPr6</sup>Sn( $\mu$ -Et)}<sub>2</sub> reported by this group.<sup>29</sup> The <sup>1</sup>H NMR spectra of **3** showed two broad resonances at  $\delta$  = 0.80–0.91 ppm and  $\delta$  = 1.23–1.29 ppm, separately, and a resolved triplet signal attributable to the two  $\alpha$ -protons of the *n*-propyl group. One-dimensional nuclear Overhauser effect spectroscopy of <sup>1</sup>H NMR spectra of **2** and **3** with selective excitation of  $\delta$  = 7.20–7.34 ppm showed transfer of nuclear spin polarization to the isopropyl substituents on the flanking rings due to the close contacts between these isopropyl groups and aromatic signals on the central phenyl ring, therefore explaining NOE-coupled multiplets of aromatic signals in **2** and **3**.

The purity of the samples of **1–4** is better represented by the <sup>13</sup>C{<sup>1</sup>H} NMR spectra, in comparison to the <sup>1</sup>H NMR spectra, where restricted rotations and NOE-couplings were present throughout the structures of **1–4**. The <sup>13</sup>C{<sup>1</sup>H} NMR spectra of **1–4** displayed two distinct chemical shifts for the carbonyl resonances in an approximate 1:4 ratio, which is consistent with their structural data (vide supra). The <sup>13</sup>C–<sup>117/119</sup>Sn coupling was not observed in all of the recorded <sup>13</sup>C{<sup>1</sup>H} NMR spectra, while <sup>13</sup>C–<sup>183</sup>W couplings were observed in the <sup>13</sup>C{<sup>1</sup>H} NMR spectra of **1** and **3** for the four equatorial carbonyl groups. The <sup>13</sup>C–<sup>183</sup>W coupling constants are <sup>1</sup>J<sub>W–C</sub> = 122 Hz, and <sup>1</sup>J<sub>W–C</sub> = 121 Hz for **1** and **3**, respectively, which is close to the reported values for L<sup>2</sup>(H)Sn–W(CO)<sub>5</sub> (L<sup>2</sup> = 2-Et<sub>2</sub>NCH<sub>2</sub>-4,6-*t*Bu<sub>2</sub>-C<sub>6</sub>H<sub>2</sub>), <sup>1</sup>J<sub>W–C</sub> = 122 Hz.<sup>24</sup> The 1:4 ratio of carbonyl resonances suggests free rotation around W–Sn bond in **1–4**. This suggests that hydridostannylene is a weak  $\pi$ -acceptor despite the presence of an empty p-orbital on the Sn atom, which is further demonstrated in calculations (vide infra). Compared to the <sup>13</sup>C{<sup>1</sup>H} NMR spectrum of **1**, <sup>13</sup>C{<sup>1</sup>H} NMR spectra of **2** and **3** showed additional signals attributable to the ethyl or *n*-propyl group coordinated at the tin atom which are similar to the reported values for tin-alkyls.<sup>29,38</sup>

The <sup>119</sup>Sn{<sup>1</sup>H} NMR spectra of **1–3** were recorded in C<sub>6</sub>D<sub>6</sub> and referenced to the external standard SnMe<sub>4</sub> in CDCl<sub>3</sub>. The <sup>119</sup>Sn signal of **1** appeared at  $\delta$  = 1159 ppm, which is slightly further upfield than  $\delta$  = 1324 ppm, the previously reported for Mo(CO)<sub>5</sub>{Sn(Ar<sup>iPr6</sup>)H}.<sup>27</sup> The <sup>119</sup>Sn signal of **1** agrees well with the <sup>119</sup>Sn NMR chemical shift of Cp<sub>2</sub>M(Ar<sup>iPr6</sup>SnH)<sub>2</sub> (M = Ti, Zr, and Hf) complexes reported by Wesemann and co-workers, which ranged from 1060 to 1250 ppm.<sup>26</sup> The <sup>119</sup>Sn{<sup>1</sup>H} NMR spectra of **2** and **3** displayed signals at  $\delta$  = 1455 ppm and  $\delta$  = 1443 ppm, respectively. Unfortunately, no <sup>119</sup>Sn signal was observed for **4**. Other reported <sup>119</sup>Sn chemical

shifts of three-coordinate tin-transition metal complexes range from 673 to 1231 ppm.<sup>45,54–58</sup>

**IR Spectroscopy.** Compounds **1–4** were further characterized by FT-IR spectroscopy. Compounds **1–3** displayed  $\nu_{\text{CO}}$  stretching bands that agree well with the previously reported complexes,<sup>27</sup> showing a characteristic pattern for a  $[\text{LM}(\text{CO})_5]$  species.<sup>59</sup> Compared to **1**, FT-IR spectra of **2** and **3** showed similar  $\nu_{\text{CO}}$  stretching bands, and disappearance of the weak absorption at  $1757\text{ cm}^{-1}$  attributed to the Sn–H stretching frequencies, as a result of olefin insertion reaction into the Sn–H bond. However, the FT-IR spectrum of **4** displayed slightly different  $\nu_{\text{CO}}$  stretching bands,  $2050\text{ cm}^{-1}$  (m),  $1963\text{ cm}^{-1}$  (m),  $1916\text{ cm}^{-1}$  (s), and  $1887\text{ cm}^{-1}$  (vs), and a weak absorption at  $1793\text{ cm}^{-1}$  for the Sn–H stretching. DFT calculations suggest similar stretching frequencies of Sn–H to the experimental values (see SI). The FT-IR spectrum of **4** is in close agreement with the values of  $\text{L}^2(\text{H})\text{Sn}\cdot\text{W}(\text{CO})_5$  ( $\text{L}^2 = 2\text{-Et}_2\text{NCH}_2\text{-4,6-}i\text{Bu}_2\text{-C}_6\text{H}_2$ ) ( $2056, 1937, 1915, 1889\text{ cm}^{-1}$  (CO), and  $1781\text{ cm}^{-1}$  (Sn–H)), reported by Jambor and co-workers.<sup>24</sup> The observed Sn–H stretching frequencies can also be compared to the reported values of the bridged-hydride Sn(II) species,  $\{\text{Ar}^{i\text{Pr}6}\text{Sn}(\mu\text{-H})\}_2$  ( $\nu_{\text{Sn-H}} = 1828$  and  $1771\text{ cm}^{-1}$ ), which are due to the asymmetric isomeric  $\{\text{Ar}^{i\text{Pr}6}\text{Sn}(\text{H})_2\text{Ar}^{i\text{Pr}6}\}$ ,<sup>10,20</sup> and terminally bound tin hydride species reported by Roesky and co-workers, as well as to  $[\{\text{HC}(\text{CMeNAr})_2\}\text{SnH}]$  ( $\text{Ar} = 2,6\text{-}i\text{Pr}_2\text{C}_6\text{H}_3$ )  $\nu_{\text{Sn-H}} = 1849\text{ cm}^{-1}$ ,<sup>11</sup>  $[\{2,6\text{-}i\text{Pr}_2\text{C}_6\text{H}_3\text{NCMe}\}_2\text{C}_6\text{H}_3\text{SnH}]$   $\nu_{\text{Sn-H}} = 1826\text{ cm}^{-1}$ ,<sup>12</sup> and  $\text{Cp}_2\text{M}(\text{Ar}^{i\text{Pr}6}\text{SnH})_2$  ( $\text{M} = \text{Ti, Zr, and Hf}$ ) complexes reported by Wesemann and co-workers, with  $\nu_{\text{Sn-H}}$  ranging from  $1741$  to  $1749\text{ cm}^{-1}$ .<sup>26</sup>

**Computational Analyses.** The structures of **1**, **2**, and **4** were further probed computationally by DFT methods and greater details are listed in the Supporting Information. Overall, the calculated gas-phase structures agreed well with the solid-state molecular structures of **1**, **2**, and **4**. In more detail, we investigated the potential reaction pathways for the ethylene insertion to complex **1** (Figure 4a), the limited conversion of **2** to **1** with  $\text{Ph}_3\text{SiH}$  (Figure 4b), and the dbu adduct formation **4** (Figure 5). First, for the ethylene insertion to **1**, it is suggested that the reaction proceeds via the initial face-on coordination of the olefin to the tin atom in **1**, the transition state for this insertion was found to be  $17.1\text{ kcal/mol}$ . The ethylene inserted product **2** was then found to be  $17.4\text{ kcal/mol}$  more stable than the starting materials **1** and  $\text{C}_2\text{H}_4$ , and therefore the overall reaction is exergonic which agrees well with the experimental findings (Scheme 3).

We investigated the catalytic potential of **1** toward hydrogenation of ethylene using NMR spectroscopy and DFT calculations, as **1** readily effects facile hydrostannylation of ethylene. Initial attempts using dihydrogen gas as the hydrogen source in the regeneration of **1** were unsuccessful; however, using  $\text{PhSiH}_3$  as the hydrogen source resulted in limited conversion of **2** to **1**. The  $^1\text{H}$  and  $^{29}\text{Si}\{^1\text{H}\}$  NMR spectra of the mixture of **2** and  $\text{PhSiH}_3$  showed signals attributable to the unreacted species, 5 min after mixing the reagents in the glove box. After 72 h at ca.  $65\text{ }^\circ\text{C}$ , the  $^1\text{H}$  NMR spectrum indicated limited conversion of **2** to **1**, as evidenced by the appearance of the  $18.62\text{ ppm}$  signal of the Sn–H in **1**. The  $^{29}\text{Si}\{^1\text{H}\}$  NMR spectrum of the reaction mixture showed only a signal for  $\text{PhSiH}_3$  even after heating for 72 h at ca.  $65\text{ }^\circ\text{C}$ . The DFT calculations suggest that the rate determining step in this transformation is the metathesis reaction between Sn–C/Si–H bond for which there is an energy barrier of  $71.3$

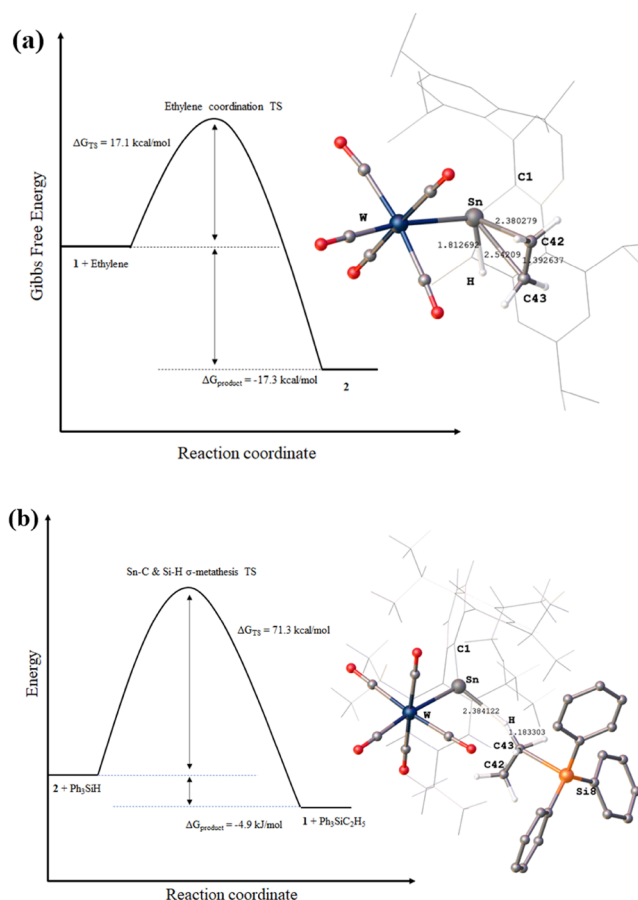


**Figure 4.** (a) DFT calculated reaction coordinate diagram of **1** +  $\text{C}_2\text{H}_4$ , with calculated gas-phase structure of the transition state;  $\text{Ar}^{i\text{Pr}6}$  is shown as wireframe. (b) DFT calculated reaction coordinate diagram of **2** +  $\text{Ph}_3\text{SiH}$ , with calculated gas-phase structure of the transition state;  $\text{Ar}^{i\text{Pr}6}$  is shown as wireframe.

$\text{kcal/mol}$ , despite the overall reaction being exergonic, albeit by just  $4.9\text{ kcal/mol}$ . Taken together the high barrier and close to thermoneutral reaction energetics, it is not surprising that the experimental conversion is very modest.

Finally, the reaction of **1** with dbu was also investigated computationally. Previously, both proton abstraction and coordination reactions have been reported to occur for dbu.<sup>22,60–62</sup> However, in the case of **1** with dbu, coordination of dbu to the tin atom in **1** was the sole reaction observed both structurally and spectroscopically. DFT calculations suggest that the proton abstraction in this system is overall endergonic by  $3.9\text{ kcal/mol}$  (compared to the free reagents **1** and dbu), yet the coordination reaction is overall exergonic by  $-14.3\text{ kcal/mol}$ . In addition, the proton abstraction transition state is at  $25.4\text{ kcal/mol}$  (compared to the adduct **4**), therefore favoring the coordination product instead of proton abstraction.

## CONCLUSIONS

Herein, we reported the synthesis of  $\text{W}(\text{CO})_5\{\text{Sn}(\text{Ar}^{i\text{Pr}6})\text{H}\}$  (**1**) via a reaction of  $\{\text{Ar}^{i\text{Pr}6}\text{Sn}(\mu\text{-H})\}_2$  with  $[\text{W}(\text{CO})_5(\text{THF})]$ . Compound **1** effects facile hydrostannylation of ethylene, or propylene, which yielded  $\text{W}(\text{CO})_5\{\text{Sn}(\text{Ar}^{i\text{Pr}6})(\text{Et})\}$ , (**2**), or  $\text{W}(\text{CO})_5\{\text{Sn}(\text{Ar}^{i\text{Pr}6})(^n\text{Pr})\}$ , (**3**). The addition of dbu, a weakly-nucleophilic base, to a solution of **1** afforded the Lewis acid–base complex  $[(\text{Ar}^{i\text{Pr}6})(\text{H})\text{Sn}(\text{dbu})\text{-W}(\text{CO})_5]$ , (**4**), which demonstrated the Lewis acidic nature of the Sn atom in **1**.



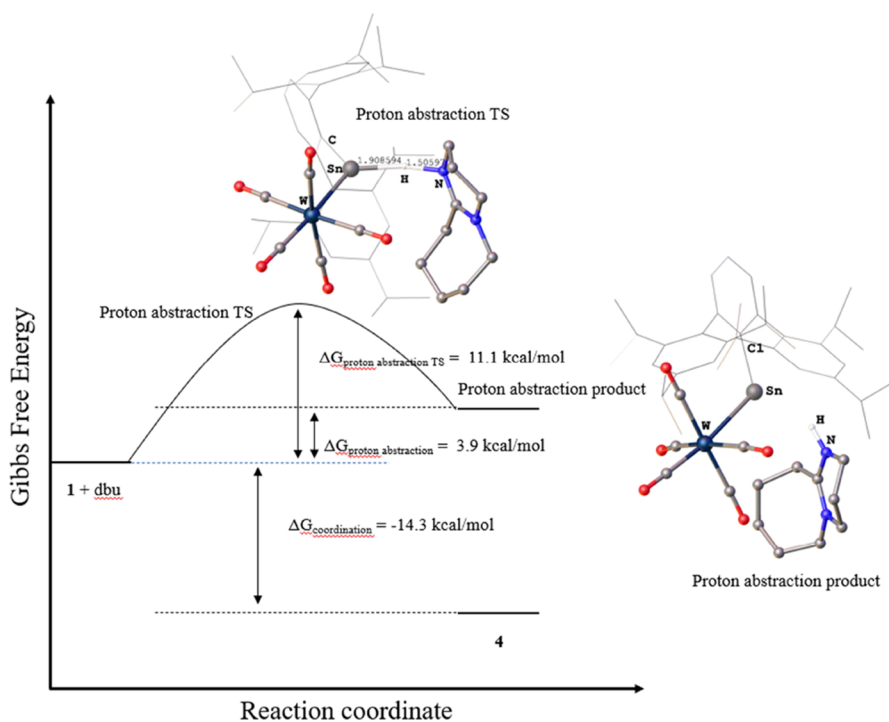
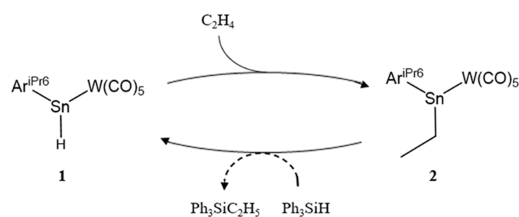


**Figure 5.** DFT calculated reaction coordinate diagram of **1** + dbu, with the calculated gas-phase structure of the transition state for proton abstraction, and calculated gas-phase structure of the proton abstraction products; Ar<sup>iPr6</sup> is shown as wireframe.

### Scheme 3. Hypothetical Catalytic Hydrosilylation of Ethylene with **1**



Investigation of the catalytic potential of **1** toward ethylene hydrosilylation by reacting **2** with PhSiH<sub>3</sub> in C<sub>6</sub>D<sub>6</sub> at elevated temperature revealed limited conversion of **2** to **1**, which was monitored by NMR spectroscopy. DFT calculations suggest that the mechanism of hydrosilylation reactions proceed via olefin insertion into the Sn–H bond by coordination of the olefin at the tin atom. The limited conversion in reaction of **2** with PhSiH<sub>3</sub> in C<sub>6</sub>D<sub>6</sub> can be associated with that the calculated rate-determining step is the metathesis reaction between Sn–C/Si–H bond with an energy barrier of 71.3 kcal/mol.

### ■ ASSOCIATED CONTENT

#### SI Supporting Information

The Supporting Information is available free of charge at <https://pubs.acs.org/doi/10.1021/acs.organomet.2c00494>.

Crystallography details, computational details, NMR, IR, and electronic spectra of the described compounds (PDF)

Optimized Cartesian coordinates (XYZ)

#### Accession Codes

CCDC 2208125–2208126 and 2208131 contain the supplementary crystallographic data for this paper. These data can be obtained free of charge via [www.ccdc.cam.ac.uk/data\\_request/](http://www.ccdc.cam.ac.uk/data_request/)

cif, or by emailing [data\\_request@ccdc.cam.ac.uk](mailto:data_request@ccdc.cam.ac.uk), or by contacting The Cambridge Crystallographic Data Centre, 12 Union Road, Cambridge CB2 1EZ, UK; fax: +44 1223 336033.

### ■ AUTHOR INFORMATION

#### Corresponding Authors

Petra Vasko – Department of Chemistry, University of Helsinki, 00014 Helsinki, Finland; [orcid.org/0000-0003-4202-6869](https://orcid.org/0000-0003-4202-6869); Email: [petra.vasko@helsinki.fi](mailto:petra.vasko@helsinki.fi)

Philip P. Power – Department of Chemistry, University of California, Davis, California 95616, United States; [orcid.org/0000-0002-6262-3209](https://orcid.org/0000-0002-6262-3209); Email: [pppower@ucdavis.edu](mailto:pppower@ucdavis.edu)

#### Authors

Qihao Zhu – Department of Chemistry, University of California, Davis, California 95616, United States

James C. Fettingner – Department of Chemistry, University of California, Davis, California 95616, United States; [orcid.org/0000-0002-6428-4909](https://orcid.org/0000-0002-6428-4909)

Complete contact information is available at:

<https://pubs.acs.org/10.1021/acs.organomet.2c00494>

#### Notes

The authors declare no competing financial interest.

### ■ ACKNOWLEDGMENTS

We are grateful for the Office of Basic Energy Sciences, U.S. Department of Energy (Grant DE-FG02-07ER4675) and the dual-source X-ray diffractometer (Grant 0840444) for financial support. P.V. would like to thank the Academy of Finland (grant numbers: 338271 and 346565), Jenny and Antti Wihuri Foundation for funding, and the CSC—IT Center for Science, Finland, for computational resources.



## REFERENCES

- (1) Hadlington, T. J.; Driess, M.; Jones, C. Low-valent group 14 element hydride chemistry: towards catalysis. *Chem. Soc. Rev.* **2018**, *47*, 4176–4197.
- (2) Hadlington, T. J.; Hermann, M.; Frenking, G.; Jones, C. Low Coordinate Germanium(II) and Tin(II) Hydride Complexes: Efficient Catalysts for the Hydroboration of Carbonyl Compounds. *J. Am. Chem. Soc.* **2014**, *136*, 3028–3031.
- (3) Hadlington, T. J.; Kefalidis, C. E.; Maron, L.; Jones, C. Efficient Reduction of Carbon Dioxide to Methanol Equivalents Catalyzed by Two-Coordinate Amido–Germanium(II) and –Tin(II) Hydride Complexes. *ACS Catal.* **2017**, *7*, 1853–1859.
- (4) Erickson, J. D.; Lai, T. Y.; Liptrot, D. J.; Olmstead, M. M.; Power, P. P. Catalytic dehydrocoupling of amines and boranes by an incipient tin(II) hydride. *Chem. Commun.* **2016**, *52*, 13656–13659.
- (5) Schneider, J.; Sindlinger, C. P.; Freitag, S. M.; Schubert, H.; Wesemann, L. Diverse Activation Modes in the Hydroboration of Aldehydes and Ketones with Germanium, Tin, and Lead Lewis Pairs. *Angew. Chem., Int. Ed.* **2017**, *56*, 333–337.
- (6) Villegas-Escobar, N.; Schaefer, H. F.; Toro-Labbé, A. Formation of Formic Acid Derivatives through Activation and Hydroboration of CO<sub>2</sub> by Low-Valent Group 14 (Si, Ge, Sn, Pb) Catalysts. *J. Phys. Chem. A* **2020**, *124*, 1121–1133.
- (7) Rivard, E.; Power, P. P. Recent developments in the chemistry of low valent Group 14 hydrides. *Dalton Trans.* **2008**, 4336–4343.
- (8) Aldridge, S.; Downs, A. J. Hydrides of the Main-Group Metals: New Variations on an Old Theme. *Chem. Rev.* **2001**, *101*, 3305–3366.
- (9) Roy, M. M. D.; Omaña, A. A.; Wilson, A. S. S.; Hill, M. S.; Aldridge, S.; Rivard, E. Molecular Main Group Metal Hydrides. *Chem. Rev.* **2021**, *121*, 12784–12965.
- (10) Eichler, B. E.; Power, P. P. [2,6-Trip<sub>2</sub>H<sub>3</sub>C<sub>6</sub>Sn(μ-H)]<sub>2</sub> (Trip = C<sub>6</sub>H<sub>2</sub>-2,4,6-i-Pr<sub>3</sub>): Synthesis and Structure of a Divalent Group 14 Element Hydride. *J. Am. Chem. Soc.* **2000**, *122*, 8785–8786.
- (11) Pineda, L. W.; Jancik, V.; Starke, K.; Oswald, R. B.; Roesky, H. W. Stable Monomeric Germanium(II) and Tin(II) Compounds with Terminal Hydrides. *Angew. Chem., Int. Ed.* **2006**, *45*, 2602–2605.
- (12) Khan, S.; Samuel, P. P.; Michel, R.; Dieterich, J. M.; Mata, R. A.; Demers, J.-P.; Lange, A.; Roesky, H. W.; Stalke, D. Monomeric Sn(II) and Ge(II) hydrides supported by a tridentate pincer-based ligand. *Chem. Commun.* **2012**, *48*, 4890–4892.
- (13) Maudrich, J.-J.; Sindlinger, C. P.; Aicher, F. S. W.; Eichele, K.; Schubert, H.; Wesemann, L. Reductive Elimination of Hydrogen from Bis(trimethylsilyl)methyltin Trihydride and Mesityltin Trihydride. *Chem. – Eur. J.* **2017**, *23*, 2192–2200.
- (14) Sindlinger, C. P.; Wesemann, L. Hydrogen abstraction from organotin di- and trihydrides by N-heterocyclic carbenes: a new method for the preparation of NHC adducts to tin(II) species and observation of an isomer of a hexastannabenzene derivative [R<sub>6</sub>Sn<sub>6</sub>]. *Chem. Sci.* **2014**, *5*, 2739–2746.
- (15) Sindlinger, C. P.; Grahneis, W.; Aicher, F. S. W.; Wesemann, L. Access to Base Adducts of Low-Valent Organotin-Hydride Compounds by Controlled, Stepwise Hydrogen Abstraction from a Tetravalent Organotin Trihydride. *Chem. – Eur. J.* **2016**, *22*, 7554–7566.
- (16) Petz, W. Transition-metal complexes with derivatives of divalent silicon, germanium, tin, and lead as ligands. *Chem. Rev.* **1986**, *86*, 1019–1047.
- (17) Filippou, A. C.; Philippopoulos, A. I.; Schnakenburg, G. Triple Bonding to Tin: Synthesis and Characterization of the Square-Pyramidal Stannylyne Complex Cation [(dppe)<sub>2</sub>W≡Sn–C<sub>6</sub>H<sub>3</sub>-2,6-Mes<sub>2</sub>]<sup>+</sup> (dppe = Ph<sub>2</sub>PCH<sub>2</sub>CH<sub>2</sub>PPh<sub>2</sub>, Mes = C<sub>6</sub>H<sub>2</sub>-2,4,6-Me<sub>3</sub>). *Organometallics* **2003**, *22*, 3339–3341.
- (18) Filippou, A. C.; Portius, P.; Philippopoulos, A. I.; Rohde, H. Triple Bonding to Tin: Synthesis and Characterization of the Stannylyne Complex trans-[Cl(PMe<sub>3</sub>)<sub>4</sub>W≡Sn–C<sub>6</sub>H<sub>3</sub>-2,6-Mes<sub>2</sub>]. *Angew. Chem., Int. Ed.* **2003**, *42*, 445–447.
- (19) Queen, J. D.; Phung, A. C.; Caputo, C. A.; Fettinger, J. C.; Power, P. P. Metathetical Exchange between Metal–Metal Triple Bonds. *J. Am. Chem. Soc.* **2020**, *142*, 2233–2237.
- (20) Rivard, E.; Fischer, R. C.; Wolf, R.; Peng, Y.; Merrill, W. A.; Schley, N. D.; Zhu, Z.; Pu, L.; Fettinger, J. C.; Teat, S. J.; Nowik, I.; Herber, R. H.; Takagi, N.; Nagase, S.; Power, P. P. Isomeric Forms of Heavier Main Group Hydrides: Experimental and Theoretical Studies of the [Sn(Ar)H]<sub>2</sub> (Ar = Terphenyl) System. *J. Am. Chem. Soc.* **2007**, *129*, 16197–16208.
- (21) Rivard, E.; Steiner, J.; Fettinger, J. C.; Giuliani, J. R.; Augustine, M. P.; Power, P. P. Convergent syntheses of [Sn<sub>7</sub>{C<sub>6</sub>H<sub>3</sub>-2,6-(C<sub>6</sub>H<sub>3</sub>-2,6-<sup>i</sup>Pr<sub>2</sub>)<sub>2</sub>}]<sub>2</sub>: a cluster with a rare pentagonal bipyramidal motif. *Chem. Commun.* **2007**, 4919–4921.
- (22) Wang, S.; Sherbow, T. J.; Berben, L. A.; Power, P. P. Reversible Coordination of H<sub>2</sub> by a Distannyne. *J. Am. Chem. Soc.* **2018**, *140*, 590–593.
- (23) Al-Rafia, S. M. I.; Malcolm, A. C.; Liew, S. K.; Ferguson, M. J.; Rivard, E. Stabilization of the Heavy Methylene Analogues, GeH<sub>2</sub> and SnH<sub>2</sub>, within the Coordination Sphere of a Transition Metal. *J. Am. Chem. Soc.* **2011**, *133*, 777–779.
- (24) Novák, M.; Dostál, L.; Růžičková, Z.; Mebs, S.; Beckmann, J.; Jambor, R. From Monomeric Tin(II) Hydride to Nonsymmetric Distannyne. *Organometallics* **2019**, *38*, 2403–2407.
- (25) Widemann, M.; Jeggle, S.; Auer, M.; Eichele, K.; Schubert, H.; Sindlinger, C. P.; Wesemann, L. Hydridotetrylene [Ar\*EH] (E = Ge, Sn, Pb) coordination at tantalum, tungsten, and zirconium. *Chem. Sci.* **2022**, *13*, 3999–4009.
- (26) Maudrich, J.-J.; Widemann, M.; Diab, F.; Kern, R. H.; Sirsch, P.; Sindlinger, C. P.; Schubert, H.; Wesemann, L. Hydridoorganostannylyne Coordination: Group 4 Metallocene Dichloride Reduction in Reaction with Organodihydridostannate Anions. *Chem. – Eur. J.* **2019**, *25*, 16081–16087.
- (27) Zhu, Q.; Fettinger, J. C.; Power, P. P. Hydrostannylation of carbon dioxide by a hydridostannylyne molybdenum complex. *Dalton Trans.* **2021**, *50*, 12555–12562.
- (28) Weiß, S.; Widemann, M.; Eichele, K.; Schubert, H.; Wesemann, L. Low valent lead and tin hydrides in reactions with heteroallenes. *Dalton Trans.* **2021**, *50*, 4952–4958.
- (29) Wang, S.; McCrea-Hendrick, M. L.; Weinstein, C. M.; Caputo, C. A.; Hoppe, E.; Fettinger, J. C.; Olmstead, M. M.; Power, P. P. Dynamic Behavior and Isomerization Equilibria of Distannenes Synthesized by Tin Hydride/Olefin Insertions: Characterization of the Elusive Monohydrido Bridged Isomer. *J. Am. Chem. Soc.* **2017**, *139*, 6586–6595.
- (30) Peng, Y.; Ellis, B. D.; Wang, X.; Fettinger, J. C.; Power, P. P. Reversible Reactions of Ethylene with Distannynes Under Ambient Conditions. *Science* **2009**, *325*, 1668–1670.
- (31) Hadlington, T. J.; Hermann, M.; Li, J.; Frenking, G.; Jones, C. Activation of H<sub>2</sub> by a Multiply Bonded Amido–Digermene: Evidence for the Formation of a Hydrido–Germene. *Angew. Chem., Int. Ed.* **2013**, *52*, 10199–10203.
- (32) Lücke, M.-P.; Yao, S.; Driess, M. Boosting homogeneous chemoselective hydrogenation of olefins mediated by a bis(silylenyl)-terphenyl-nickel(0) pre-catalyst. *Chem. Sci.* **2021**, *12*, 2909–2915.
- (33) Glaser, P. B.; Tilley, T. D. Catalytic Hydrosilylation of Alkenes by a Ruthenium Silylene Complex Evidence for a New Hydro-silylation Mechanism. *J. Am. Chem. Soc.* **2003**, *125*, 13640–13641.
- (34) Wu, J.; Thiyagarajan, S.; Fonseca Guerra, C.; Eduard, P.; Lutz, M.; Noordover, B. A. J.; Koning, C. E.; van Es, D. S. Isohexide Dinitriles: A Versatile Family of Renewable Platform Chemicals. *ChemSusChem* **2017**, *10*, 3202–3211.
- (35) Pangborn, A. B.; Giardello, M. A.; Grubbs, R. H.; Rosen, R. K.; Timmers, F. J. Safe and Convenient Procedure for Solvent Purification. *Organometallics* **1996**, *15*, 1518–1520.
- (36) Boylan, M. J.; Braterman, P. S.; Fullarton, A. Metal carbonyl photolysis and its reversal; probable spurious nature of “trigonal bipyramidal Mo(CO)<sub>5</sub>”. *J. Organomet. Chem.* **1971**, *31*, C29–C30.
- (37) Pu, L.; Twamley, B.; Power, P. P. Terphenyl Ligand Stabilized Lead(II) Derivatives of Simple Organic Groups: Characterization of Pb(R)C<sub>6</sub>H<sub>3</sub>-2,6-Trip<sub>2</sub> (R = Me, t-Bu, or Ph; Trip = C<sub>6</sub>H<sub>2</sub>-2,4,6-i-Pr<sub>3</sub>), {Pb(μ-Br)C<sub>6</sub>H<sub>3</sub>-2,6-Trip<sub>2</sub>}, py-Pb(Br)C<sub>6</sub>H<sub>3</sub>-2,6-Trip<sub>2</sub> (py = Pyri-

- dine), and the Bridged Plumblyne Complex  $[\{W(CO)_4\}_2(\mu-Br)(\mu-PbC_6H_3-2,6-Trip_2)]$ . *Organometallics* **2000**, *19*, 2874–2881.
- (38) Hadlington, T. J.; Hermann, M.; Frenking, G.; Jones, C. Two-coordinate group 14 element(II) hydrides as reagents for the facile, and sometimes reversible, hydrogermylation/hydrostannylation of unactivated alkenes and alkynes. *Chem. Sci.* **2015**, *6*, 7249–7257.
- (39) Pyykkö, P.; Atsumi, M. Molecular Single-Bond Covalent Radii for Elements 1–118. *Chem. – Eur. J.* **2009**, *15*, 186–197.
- (40) Lappert, M. F.; Power, P. P.; Slade, M. J.; Hedberg, L.; Hedberg, K.; Schomaker, V. Monomeric bivalent group 4B metal dialkylamides  $M[N(CMe_2)(CH_2)_3CMe_2]_2$  ( $M = Ge$  or  $Sn$ ), and the structure of a gaseous disilylamide,  $Sn[N(SiMe_3)_2]_2$ , by gas electron diffraction. *J. Chem. Soc., Chem. Commun.* **1979**, 369–370.
- (41) Mansell, S. M.; Russell, C. A.; Wass, D. F. Synthesis and Structural Characterization of Tin Analogues of N-Heterocyclic Carbenes. *Inorg. Chem.* **2008**, *47*, 11367–11375.
- (42) Mansell, S. M.; Herber, R. H.; Nowik, I.; Ross, D. H.; Russell, C. A.; Wass, D. F. Coordination Chemistry of N-Heterocyclic Stannylenes: A Combined Synthetic and Mössbauer Spectroscopy Study. *Inorg. Chem.* **2011**, *50*, 2252–2263.
- (43) Jambor, R.; Kašná, B.; Koller, S. G.; Strohmann, C.; Schürmann, M.; Jurkschat, K.  $[\{2,6-(Me_2NCH_2)_2C_6H_3(H_2O)Sn\}W(CO)_5]^+ \cdot CB_{11}H_{12}^-$ : Aqua Complex of a Transition-Metal-Bound Organotin(II) Cation versus an Ammonium-Type Structure. *Eur. J. Inorg. Chem.* **2010**, 902–908.
- (44) Balch, A. L.; Oram, D. E. Four- and five-coordinate tin(II) (stannylene) compounds: crystal and molecular structures of  $W(CO)_5\{SnCl_2(OC_4H_8)\}$  and  $W(CO)_5\{SnCl_2(OC_4H_8)_2\}$ . *Organometallics* **1988**, *7*, 155–158.
- (45) Weidenbruch, M.; Stilter, A.; Schlaefke, J.; Peters, K.; Schnering, H. G. Compounds of germanium and tin XIV. Rearrangement of bis(2,4,6-tri-tert-butylphenyl)stannylene: synthesis and structure of a donor-free alkylarylstannylene-tungsten complex. *J. Organomet. Chem.* **1995**, *501*, 67–70.
- (46) Kašná, B.; Jambor, R.; Schürmann, M.; Jurkschat, K. Synthesis and characterization of novel intramolecularly O,C,O-coordinated heteroleptic organostannylenes and their tungstenpentacarbonyl complexes. *J. Organomet. Chem.* **2008**, *693*, 3446–3450.
- (47) Jambor, R.; Herres-Pawlis, S.; Schürmann, M.; Jurkschat, K.  $[\{2,6-(Me_2NCH_2)_2C_6H_3\}Sn(\mu-OH)W(CO)_5]_2$ : A Transition-Metal-Coordinated Organotin(II) Hydroxide. *Eur. J. Inorg. Chem.* **2011**, *2011*, 344–348.
- (48) Hashimoto, H.; Nagata, K. Transition-metal Complexes with Triple Bonds to Si, Ge, Sn, and Pb and Relevant Complexes. *Chem. Lett.* **2021**, *50*, 778–787.
- (49) Lebedev, Y. N.; Das, U.; Schnakenburg, G.; Filippou, A. C. Coordination Chemistry of  $[E(\text{Idipp})]^{2+}$  Ligands ( $E = Ge, Sn$ ): Metal Germylidyne  $[Cp^*(CO)_2W\equiv Ge(\text{Idipp})]^+$  and Metallotetraylene  $[Cp^*(CO)_3W-E(\text{Idipp})]^+$  Cations. *Organometallics* **2017**, *36*, 1530–1540.
- (50) Eichler, B. E.; Phillips, A. D.; Haubrich, S. T.; Mork, B. V.; Power, P. P. Synthesis, Structures, and Spectroscopy of the Metallostannylenes  $(\eta^5-C_5H_5)(CO)_3M-\ddot{S}n-C_6H_3-2,6-Ar_2$  ( $M = Cr, Mo, W$ ;  $Ar = C_6H_2-2,4,6-Me_3, C_6H_2-2,4,6-Pr^i_3$ ). *Organometallics* **2002**, *21*, 5622–5627.
- (51) McCrea-Hendrick, M. L.; Caputo, C. A.; Linnner, J.; Vasko, P.; Weinstein, C. M.; Fettinger, J. C.; Tuononen, H. M.; Power, P. P. Cleavage of Ge–Ge and Sn–Sn Triple Bonds in Heavy Group 14 Element Alkyne Analogues  $(EAR^{iPr^4})_2$  ( $E = Ge, Sn$ ;  $Ar^{iPr^4} = C_6H_3-2,6(C_6H_3-2,6-Pr^i_2)$ ) by Reaction with Group 6 Carbonyls. *Organometallics* **2016**, *35*, 2759–2767.
- (52) Hayes, P. G.; Gribble, C. W.; Waterman, R.; Tilley, T. D. A Hydrogen-Substituted Osmium Stannylene Complex: Isomerization to a Metallostannylene Complex via an Unusual  $\alpha$ -Hydrogen Migration from Tin to Osmium. *J. Am. Chem. Soc.* **2009**, *131*, 4606–4607.
- (53) Vicha, J.; Marek, R.; Straka, M. High-Frequency  $^1H$  NMR Chemical Shifts of SnII and PbII Hydrides Induced by Relativistic

Effects: Quest for PbII Hydrides. *Inorg. Chem.* **2016**, *55*, 10302–10309.

(54) Weidenbruch, M.; Stilter, A.; Peters, K.; von Schnering, H. G. Verbindungen des Germaniums und Zinns. Alkylarylstannylene-Komplexe des Chroms und Molybdäns ohne Donorstabilisierung. *Z. Anorg. Allg. Chem.* **1996**, *622*, 534–538.

(55) Weidenbruch, M.; Stilter, A.; Saak, W.; Peters, K.; von Schnering, H. G. An octahedral stannylmanganese stannylene complex. *J. Organomet. Chem.* **1998**, *560*, 125–129.

(56) Schneider, J. J.; Czap, N.; Bläser, D.; Boese, R. Metal Atom Synthesis of  $(\eta^6\text{-Toluene})(\eta^2\text{-ethene})\text{iron}(\sigma^1\text{-stannandiyl})$ : Unusual Iron(0) Complexes. *J. Am. Chem. Soc.* **1999**, *121*, 1409–1410.

(57) Bareš, J.; Richard, P.; Meunier, P.; Pirio, N.; Padělková, Z.; Cernošek, Z.; Cisařová, I.; Růžicka, A. Reactions of C,N-chelated Tin(II) and Lead(II) Compounds with Zirconocene Dichloride Derivatives. *Organometallics* **2009**, *28*, 3105–3108.

(58) Schneider, J. J.; Czap, N.; Bläser, D.; Boese, R.; Ensling, J.; Gütlisch, P.; Janiak, C. Experimental and Theoretical Investigations on the Synthesis, Structure, Reactivity, and Bonding of the Stannylene-Iron Complex Bis{bis(2-tert-butyl-4,5,6-trimethyl-phenyl)}Sn}Fe( $\eta^6\text{-toluene}$ ). *Chem. – Eur. J.* **2000**, *6*, 468–474.

(59) Kircher, P.; Huttner, G.; Heinze, K.; Schiemenz, B.; Zsolnai, L.; Büchner, M.; Driess, A. Four-Coordinate Group-14 Elements in the Formal Oxidation State of Zero – Syntheses, Structures, and Dynamics of  $[\{(CO)_5Cr\}_2Sn(L_2)]$  and Related Species. *Eur. J. Inorg. Chem.* **1998**, *1998*, 703–720.

(60) Wang, P.; Zhang, M.; Zhu, C. Synthesis, Characterization, and Reactivity of a Pincer-Type Aluminum(III) Complex. *Organometallics* **2020**, *39*, 2732–2738.

(61) Sole, R. D.; Luca, A. D.; Mele, G.; Vasapollo, G. First evidence of formation of stable DBU Zn-phthalocyanine complexes: synthesis and characterization. *J. Porphyrins Phthalocyanines* **2005**, *09*, S19–S27.

(62) Agou, T.; Ikeda, S.; Sasamori, T.; Tokitoh, N. Synthesis and Structure of Lewis Base-Coordinated Phosphanylaluminanes Bearing P–H and Al–Br Moieties. *Eur. J. Inorg. Chem.* **2018**, 1984–1987.

## Recommended by ACS

### Synthesis of Mo(IV) *para*-Substituted Styrene Complexes and an Exploration of Their Conversion to 1-Phenethylidene Complexes

Sumeng Liu, Richard R. Schrock, *et al.*

NOVEMBER 23, 2022  
ORGANOMETALLICS

READ 

### Beyond $N\{N(SiMe_3)_2\}_2$ : Synthesis of a Stable Solvated Sodium Tris-Amido Nickelate

Andry M. Borys and Eva Hevia

JANUARY 17, 2021  
ORGANOMETALLICS

READ 

### Pursuit of an Electron Deficient Titanium Nitride

Lauren N. Grant, Daniel J. Mindiola, *et al.*

APRIL 07, 2021  
INORGANIC CHEMISTRY

READ 

### Halide Effects in Reductive Splitting of Dinitrogen with Rhenium Pincer Complexes

Richt S. van Alten, Sven Schneider, *et al.*

JULY 21, 2022  
INORGANIC CHEMISTRY

READ 

Get More Suggestions >